Crystals based on solid solution of $Ag_{1-x}Tl_xBr_{1-x}I_x$ for the manufacturing of IR fibers

Alexandr Korsakov, Liya Zhukova*, Dmitrii Salimgareev, and Vladislav Zhukov

Ural Federal University named after the first President of Russia, B.N. Yeltsin. 19 Mira Street, Ekaterinburg 620002, Russia

**Corresponding author: l.v.zhukova@urfu.ru*

Received April 9, 2015; accepted June 8, 2015; posted online July 23, 2015

For the development of fiber optics for the range from 0.2 to 50.0 μm, one needs light-stable, nonhygroscopic, ductile crystals that would be transparent within this spectral range and have a lack of cleavage, and from which the flexible infrared (IR) fibers are extruded. The crystals based on solid solutions of silver and monadic thallium halides meet the conditions listed above. Consequently, by differential thermal and x ray analyses, we study the TlBr–TlI phase diagram using the crystals with optimal compositions, which we grow ourselves. We also manufacture light-stable nanocrystalline IR fibers that are transparent at longer wavelengths compared with AgCl–AgBr fibers.

OCIS codes: 060.2390, 160.4670, 260.1180.
doi: 10.3788/COL201513.090602.

Among all the crystals being explored nowadays and used in the mid-infrared (IR) range, the ones based on solid silver and monadic thallium halide solutions have the greatest potential[1]. The former are represented mainly by the AgCl–AgBr system, which the flexible IR fibers are extruded from, and they are the only nontoxic polycrystalline fibers that can operate from 2.0 up to 30.0 μm[2–5]. They have found their applications in IR spectroscopy, laser diagnostic and endoscopic medicine, and laser cutting and welding, as well as in low-temperature pyrometry for night-vision fiber-optical system manufacturing[6–8]. However, the application is constrained by their light sensitivity, which leads directly to the deterioration of the optical properties and affects the diffusion at the core-cladding interface when extruding double-layer fibers. The second system is particularly represented by monovalent thallium halide crystals of TlBr–TlI (KRS-5) and the optical fibers based on them. This system is characterized by both high cleavage and grain recrystallization, the latter implying a coarse-grained microstructure, which scatters light rather strongly and thereat does limit their fiber-optical applications despite the properties of radiation resistance and wide spectral range of transparency.

Therefore, for operations within the range of 2.0–40.0 μm, we developed IR fibers based on solid solutions of crystals to substitute for AgBr-TlI[9–12]. This choice was justified by such factors as the pairwise charge equality of the Ag^+ and Tl^+, and Br^- and I^- ions, the size proximity of their ionic radii, and the closeness of their crystal lattice parameters. Furthermore, the phase diagrams of AgCl–AgBr and TlBr–TlI proved to support a continuous number of unlimited, mutually soluble solid solutions with a lower melting point of 412°C, compared with that of the initial components. This value also corresponds to the melting points of $AgCl_{0.25}Br_{0.75}$ and $TlBr_{0.46}I_{0.54}$ (KRS-5). They possess similar physico-chemical properties; therefore, it was of interest to investigate the possibility of obtaining the crystals from the solid solutions based on these systems.

The nontrivial phase equilibrium diagram of the AgBr-TlI systems has been investigated using differential thermal and x ray phase analysis. For its construction, the thermal effects obtained under cooling were used, since they allow for the representation of a realistic picture of crystallization.

Regarding the samples, we used high-purity silver bromide and thallium iodide with the impurity content of 1×10^{-6} wt.%. Compositions with TlI content in AgBr from 0 to 100 wt.% with a 10% increment have previously been studied[11]. It is known that silver bromide (bromargyrite mineral) has a cubic NaCl modification below 259°C, and an orthorhombic one above 259°C. The two-component "thallium–iodine" phase diagram is characterized by a number of polymorphic transformations at 178°C and 230°C. There are two modification for the β TI phase: when the melt is cooled to a temperature of 230°C, the β_1 phase (TlI) turns into a cubical β_2 phase (TlI) of the CsCl type, and below 178°C, the β_2 phase is converted into an orthorhombic $\beta 3$ phase (TlI). Similar transformations are also observed at the same temperatures for the AgBr-TlI system (see Fig. 1).

In the absence of external fields, we accept that the thermodynamic state of the system is determined by the temperature and static pressure. The diagram shows that there is a region of limited solubility when the TlI content in AgBr exceeds 25 wt.%. These halides form the eutectic system with a eutectic point at nearly 160°C with TlI content of 60 wt.%. To define the eurectic point precisely, the Tamman triangle was built based on certain thermal effects (see Fig. 1). The peak magnitudes of the thermal effects were placed on the liquidus line for the phase compositions with a TlI content of 32, 40, 50, 60,

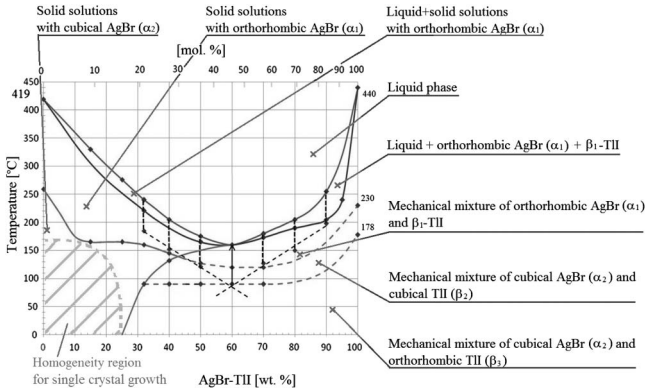

Fig. 1. AgBr-TlI phase diagram.

70, 80, and 90 wt.%. Through these points, dotted lines were drawn; these are the lateral sides of the Tamman triangle. Their intersection point confirmed the presence of a eutectic point in the AgBr-TI system with the content of TlI at 60 wt.% and a temperature of 160°C.

The liquidus line consists of two parts. The left one stands for the chilling line of the α_1 phase (orthorhombic solid solutions of various compositions up to 60 wt.% of TlI in AgBr). After cooling down further, the α_1 phase changes into the α_2 phase (cubic NaCl-type solid solutions) due to polymorphic transformation, which is confirmed by x ray analysis (see Fig. 2). The transformation line exists at around 165°C, when the cubic solid solutions (the α_2 phase) are in equilibrium with the orthorhombic ones (the α_1 phase), which, in their turn, are in equilibrium with the liquid phase.

In the rightmost part of the diagram, there is a region where the $\alpha_1 + \beta_1$ mechanical mixture exists due to the polymorphic transformations of TlI (the β_1, β_2, and β_3 phases). When chilled to below 230°C, the mixture turns into the $\alpha_2 + \beta_2$ phase. It turns into the $\alpha_2 + \beta_3$ phase below 178°C. Thus, one can conclude that AgBr lattice may accommodate up to 25 wt.% of TlI. At higher contents, it seems impossible to grow single crystals within the corresponding region of the T-x diagram.

We experimentally proved the phase diagram's competence to demonstrate the optimal single crystal growing regimes in dynamic mode when the $Ag_{1-x}Tl_xBr_{1-x}I_x$ is melting congruously within the concentration range from 0 up to 25 wt.% (14 mol.%). To achieve the certain physical and chemical properties demanded in practice, the mandatory condition for the batch is its chemical homogeneity. Such a uniform batch was obtained in the form of a homogeneous solid solution by means of a hydrochemical technique called thermal-zone crystallization-synthesis, which did not result in the decomposition of light-sensitive materials like silver and monadic thallium halides[12].

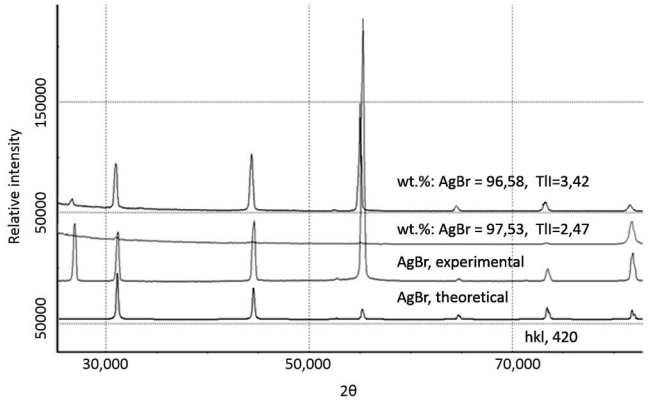

Fig. 2. X ray of AgBr and solid solutions of AgBr–TlI.

In order to grow the single crystals, we constructed a growing unit (KPCh-02) that fulfilled the Bridgman–Stockbarger technique with melt axial vibration[12]. For the system in question—AgBr-TlI—the thallium iodide content in the single crystals obtained varied from 1 up to 25 wt.% (14 mol.%). The ampoule velocity was 0.6–0.9 mmph depending on the composition. The thermal regimes were matched experimentally according to the crystal chemical composition and covered the region from 235°C to 410°C. The higher temperatures corresponded to the lower thallium halide concentrations in the solid solutions.

From the crystals grown, the nanocrystalline IR fibers were extruded with increased light stability and hardness; their optical losses proved to amount to 0.1–0.5 dB/m at 10.6 μm, with a transmission range from 2 up to 40 μm.

At longer wavelengths, light attenuation is due to Raleigh scattering, which depends on the refractive index inconstancy due to its density fluctuation and on the composition, and decreases dramatically with the increase of the wavelength. There exists a certain dependence of the electromagnetic radiation absorption on the grain size and the composition of the polycrystalline material, which the radiation passes through. To determine this relationship, we used IR fibers of three compositions. Their transmission spectra (see Fig. 3) were recorded using a Fourier

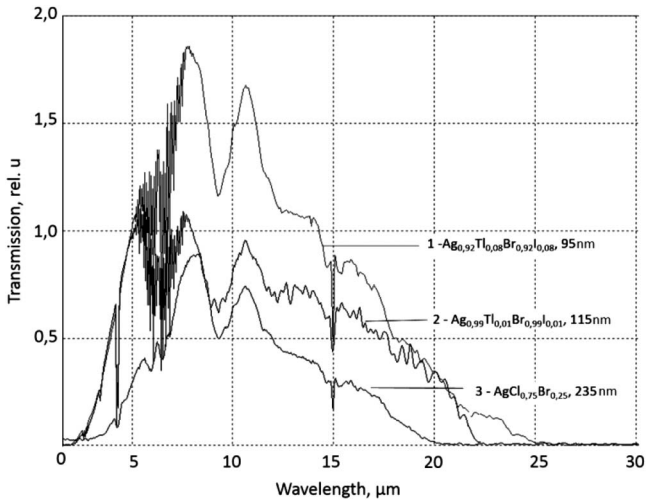

Fig. 3. Transmission spectra of three 0.5 m-long IR fibers; the spectra depend on the average grain size. The high frequency fluctuations around 6–7 μm are due to water absorption.

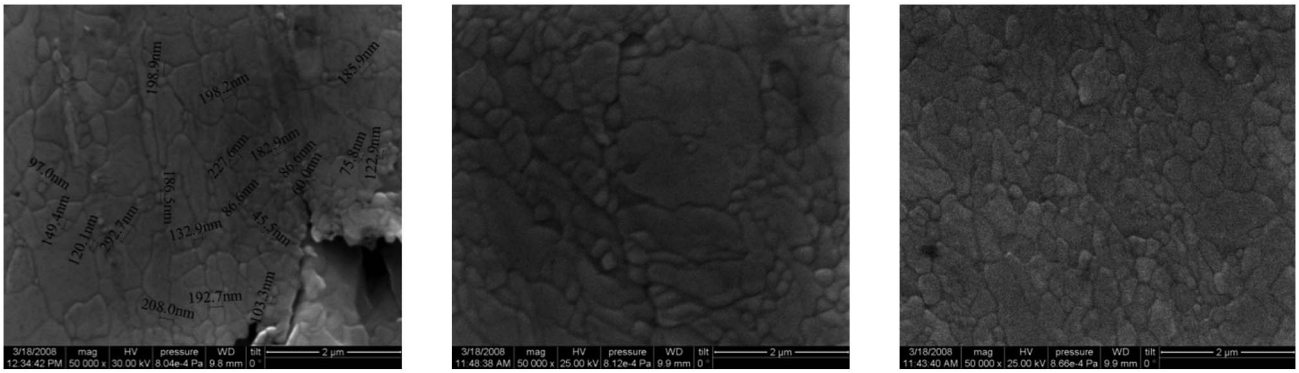

Fig. 4. Fiber cross-section SEM images (for content, see Fig. 3). Average grain size: (a) 237, (b) 115, and (c) 95 nm.

transform IR unit IRAfinity-21 (Shimadzu) with a KBr divider within the range from 1.28 to 28.7 μm. The fiber lengths were all 0.5 m.

As is seen from Fig. 3, within the wavelength range in question, the better transmission is that of the $Ag_{0.92}Tl_{0.08}Br_{0.92}I_{0.08}$ fiber formed by the 95 nm-sized grains. Figure 4 demonstrates the scanning electron microscope (SEM) images of the IR fibers depending on the extrusion regimes and crystal composition. The fiber depicted in Fig. 4(a) is $AgCl_{0.75}Br_{0.25}$ at the extrusion temperature of 170°C and is under the pressure of 1100 MPa onto a 10 mm bullet. The fibers in Figs. 4(b) and 4(c) are made of $Ag_{0.99}Tl_{0.01}Br_{0.99}I_{0.01}$ and $Ag_{0.92}Tl_{0.08}Br_{0.92}I_{0.08}$, and the temperatures are 180°C and 190°C and the pressures are 950 and 800 MPa onto the 10 mm bullet, respectively. The SEM images were collected via scanning electron microscope FEI CM 30 with secondary electron registration. The unit allows for 100000-fold magnification. The mean grain size estimation was carried out via the CellSens Standart software.

Thus, we studied and built a nontrivial AgBr-TlI phase diagram that is characterized by its wide homogeneous region. For this system, the homogeneous region—particularly, the T-x range where the cubic substitution solid solution with Fm3m symmetry exists—spans up to 25 wt.% (14 mol.%). These results are confirmed by the x ray analysis.

On the basis of the phase diagrams, we use the Bridgman–Stockbarger technique to grow single crystals made of the compositions above, which verifies the diagram's competency. We extrude the IR fibers from these crystals and determine the radiation absorption dependence on the grain size and the composition of the polycrystalline material. We figure out that the $Ag_{0.92}Tl_{0.08}Br_{0.92}I_{0.08}$ fiber with the mean grain size of 95 nm possesses the best spectral transmission compared to the other samples.

References

1. A. S. Korsakov, L. V. Zhukova, E. A. Korsakova, V. V. Zhukov, and V. S. Korsakov, Tsvetnye Metally 62 (2013).
2. V. G. Artjushenko, L. N. Butvina, V. V. Vojtsekhovsky, E. M. Dianov, and J. G. Kolesnikov, Proc. Soc. Photo-Opt. Instrum. Eng. **843**, 155 (1988).
3. T. Katsuyama and H. Matsumura, *Infrared Optical Fibers* (Mir, 1992).
4. M. Platkov, A. Tsun, L. Nagli, and A. Katzir, Rev. Sci. Instrum. **77**, 126103 (2006).
5. A. Ksendzov, T. Lewi, O. P. Lay, S. R. Martin, R. O. Gappinger, P. R. Lawson, R. D. Peters, S. Shalem, A. Tsun, and A. Katzir, Appl. Opt. **47**, 5728 (2008).
6. L. Zhukova, A. Korsakov, A. Chazov, D. Vrublevsky, and V. Zhukov, Appl. Opt. **51**, 2414 (2012).
7. A. Chazov, A. Korsakov, L. Zhukova, D. Vrublevsky, V. Zhukov, and S. Kortov, in *Advanced Photonics Congress, Nonlinear Photonics Conference* (2012), paper STu3F.3.
8. A. Chazov, L. Zhukova, D. Vrublevsky, V. Korsakov, V. Zhukov, and N. Terlyga, in *Advanced Photonics Congres, Nonlinear Photonics Conference* (2012), paper SM2E.3.
9. A. Korsakov, L. Zhukova, D. Vrublevsky, A. Chazov, V. Korsakov, and V. Kortov, in *Imaging and Applied Optics Congress* (2013), paper FTu3D.5.
10. L. V. Zhukova, N. V. Primerov, A. S. Korsakov, and A. I. Chazov, Inorg. Mater. **44**, 1372 (2008).
11. A. Korsakov, L. Zhukova, E. Korsakova, and E. Zharikov, J. Cryst. Growth **386**, 94 (2014).
12. Tel Aviv University, Web site of the research team "The Applied Physics Group," Invisible Obstacles, http://www.tau.ac.il/~applphys/ (10 March 2015).